Remaining Useful Life Estimation of Hydrokinetic Turbine Blades Using Power Signal

Yu Huang, Yufei Tang, and James VanZwieten
Florida Atlantic University
Boca Raton, FL 33431, USA
Email: {yhwang2018, tangy, jvanzwi}@fau.edu

Guoqian Jiang
Yanshan University
Qinhuangdao, Hebei 066004, China
Email: jgqysu@gmail.com

Tao Ding
Xi'an Jiaotong University
Xian, Shaanxi 710049, China
Email: tding15@mail.xjtu.edu.cn

***Abstract*—Marine hydrokinetic (MHK) turbines extract renewable energy from harsh marine environments, where biofouling and corrosion acting on turbine blades will affect system performance and lead to progressively increasing damages. Thus, accurately estimating a blade's remaining useful life (RUL) is important to achieving condition-based maintenance to ensure secure and reliable operations of MHK turbines, and the reduced cost of hydrokinetic power. In this paper, we propose a new RUL estimation method based on adaptive neuro-fuzzy inference system (ANFIS) and particle filtering (PF) approaches, establishing a relationship between blade imbalance faults and the produced power signal. The ANFIS is trained via historical failure data, and it constitutes with a m-order hidden Markov model to describe the fault propagation process. The high-order particle filter uses this Markov model to predict RUL in the form of a probability density function through collected normalized time series data. Results demonstrate the strong potential of the proposed approach for MHK turbine lifetime prediction.**

I. INTRODUCTION

Recently, marine hydrokinetic (MHK) energy production, with the advantages including high power potential and the predictability of tidal/ocean currents, is becoming a welcome alternative to the use of fossil fuels for electrical power generation on large scales [1]. However, MHK turbines usually work in harsh marine environments [2] with challenges such as biofouling and corrosion potentially inducing additional faults. Corrosion and marine organisms (or pollutants) that become attached to moving parts can lead to imbalance faults (i.e., mass or hydrodynamics of blades no longer being equal), resulting in the dynamic asymmetry of torque on the rotating shaft. Blade imbalances reduce overall performances, and if not detected and dealt with in a timely manner may further damage MHK turbines or even lead to an interruption of power generation. Therefore, it is highly desired to detect blade imbalance faults at an early stage to prevent further deterioration, reducing maintenance costs and downtime of MHK turbines.

The knowledge of equipment health status and future evolution prediction are at the basis of condition based maintenance strategies [3]. While traditional strategies such as breakdown corrective maintenance and scheduled preventive maintenance are becoming less capable of meeting the increasing industrial demand of efficiency and reliability, intelligent prognostic and health management (PHM) technologies are showing promising abilities. Remaining useful life (RUL) estimation is an indispensable part in PHM. The RUL is certainly a random variable, depending on the current device state and operating environment. Researchers refer the estimation of device RUL, in a probabilistic way, to the formulation and estimation of the probability density function of x_t conditional based on Y_t, denoted as $f(x_t|Y_t)$ or $E(x_t|Y_t)$, where x_t defined as the random variable of the RUL at time t, Y_t is the historic operational profiles and condition monitoring data up to t. For the case without the influence of Y_t, the estimation of $f(x_t|Y_t)$ is trivial since [4]:

$$f(x_t|Y_t) = f(x_t) = \frac{f(t+x_t)}{R(t)} \tag{1}$$

where $R(t)$ is the survival function at t.

Generally, there are two main categories of data for RUL prediction in PHM: event data and condition monitoring (CM) data [5]. Event data is recorded when the failures occurred in the past, which is scarce due to situations not being able to run-to-failure (i.e., measurements are not available to fully capture the sequence of the events leading to failure). In contrast, CM data is versatile and is easily and directly linked with RUL prediction, such as monitored data and degradation signals. Using these two types of data, existing methods for RUL estimation in PHM can be grouped into the following three categories: model-based [6], data driven [7] and hybrid approaches [8]. Model-based approaches, such as Weibull distribution, require extensive prior knowledge to precisely model the complex system degradation, which is usually unavailable in practice [9]. In data driven approaches, including neural network (NN), support vector machine (SVM) and hidden Markov models, the degradation is modeled based on historical data. Hybrid approaches aim to combine both advantages, but still remain complex to develop.

Recently, mapping monitored feature data to corresponding RUL using data-driven approaches has received increasing attention, especially neural network-based approaches [10], [11]. The integration of neural networks and fuzzy systems has been employed successfully in the prediction of system health condition degradation [12], [13]. To improve the prediction accuracy in real applications, where fault degradation is a complex nonlinear problem and updating system states in real time via new data is required, this has been coupled with sequential Monte Carlo methods such as particle filtering [14], [15].

In this paper, the MHK turbine RUL estimation is investigated. Because of the high nonlinearity of this problem, the first-order hidden Markov model (HMM) is not gener-

978-1-7281-1981-6/19/$31.00 ©2019 IEEE

ally applicable, and a high-order model is more appropriate to describe the MHK blade fault growth trend. The major contribution of this paper is two-fold:

1) A new form of Noise-to-Signal Ratio (NSR) fault feature is defined based on the collected generator power signal to represent the degradation of MHK turbine blades and for fault prognosis and RUL prediction.
2) An adaptive neurofuzzy inference systems (ANFIS) and 4th-order particle filter (PF) based framework is proposed to obtain the RUL in probability density function (PDF) form with respect to each time step signal, which possesses merits including nonlinear mapping and real-time state estimation.

The rest of this paper is organized as follows: Section II introduces the theoretical analysis of features in generator power signals that are induced by blade faults. Section III presents the proposed fault prognostic and RUL prediction method. Section IV reports the validation results of the proposed approach using data obtained from a blade run-to-failure test. Section V provides concluding remarks.

II. POWER SIGNAL FAULT FEATURE ANALYSIS

In this paper, we mainly focused on permanent magnet synchronous generators (PMSG) based MHK generation system [16]. Due to the electro-mechanical coupling between generator and rotating components, the vibrations of the drivetrain induced by an imbalance fault in the blade will modulate the current signals of the generator, considering the transition from current to power (i.e., P=V∗I), making it possible to use generator power signals to conduct blade fault prognosis.

A. Signal Conditioning

When a faulty turbine with constant load and speed, the air gap torque of the generator T_e consists of a constant component T_{eo} and an oscillatory component at fault characteristic frequency f_i and phase φ_i:

$$T_e = T_{eo} + \sum T_i cos(2\pi f_i t + \varphi_i) \tag{2}$$

In a synchronously rotating reference frame, the stator currents can be decomposed into two components: a magnetizing component i_{sM}, which is zero when the PMSG operates with a unity power factor, and a torque producing component i_{sT}, which can be written as:

$$i_{sT} = i_{sTo} + \sum A_{sTi} cos(2\pi f_i t + \varphi_{Ti}) \tag{3}$$

where i_{sT} is the torque producing stator current of the PMSG, consisting of average value of torque producing current i_{sTo} and torque producing current at the characteristic frequency f_i with associated amplitude A_{sTi} and phase φ_{Ti}.

Let's consider a periodic current signal i_{sT} with period T_0. The power of this signal over all periods is given by:

$$P = \lim_{n\to\infty} \frac{nE_1}{nT_0} = \int_{-\frac{T_0}{2}}^{\frac{T_0}{2}} |i_{sT}(t)|^2 \, dt \tag{4}$$

where E_1 is the signal energy in one period. This calculated power P is directly related with the measured generator power.

For the MHK turbine health condition monitoring, the power signal collected from the generator usually have low signal-to-noise ratios because the blade imbalance fault related information is typically weak in the power signals, particularly when the fault is in initial stage. To overcome this short, high-frequency sampling noise in power signal needs to be filtered out. Then, the power spectral density (PSD) of the processed signal is calculated and the fault feature is extracted from the PSD spectrum for fault prognosis and RUL prediction.

B. Fault Feature Extraction

Around the fundamental frequency of f in the power signal, the amplitudes at both the fundamental frequency f and original sidebands at characteristic frequency f_i will change when an imbalanced fault occurs, along with new sidebands excited. Therefore, the fluctuation of power at the fundamental frequency and the sidebands can indicate the degradation of blade imbalance. To specify, define noise-to-signal ratio (NSR) as the characteristic feature associated with blade imbalance fault:

$$NSR = \frac{P_{noise}}{P_{signal}} = \frac{P_{total} - P_{signal_o}}{P_{signal}} \tag{5}$$

where $P_{noise} = P_{total} - P_{signalo}$, P_{signal_o} is the power of fundamental frequency component (i.e., the amplitude at the fundamental frequency of the PSD spectrum) at healthy state, P_{total} is the total power of the signal at current state (i.e., fault state) and P_{signal} is the fundamental frequency component of the signal at current state.

When the NSR reaches a threshold, we can regard this as a failure state. The threshold ξ can be calculated as the average value of the NSRs of available imbalance fault cases:

$$\xi = \frac{1}{N} \sum_{i=1}^{N} NSR_i \tag{6}$$

where N is the number of the total collected datasets.

III. PROPOSED RUL PREDICTION FRAMEWORK

Fig. 1 presents the flowchart of the framework for RUL prediction, where fault feature NSR is extracted and defined as the state x of the turbine health condition; The ANFIS learns the degradation model of the fault feature; The PF is applied to obtain the PDF of the RUL for turbine with blade imbalance fault based on the learned degradation model and new measurements.

A. Degradation Modeling using ANFIS

The ANFIS uses the current and previous state measurements as inputs to learn the transition function, calculating the output at next time instant. Instead of using a first order model, a nth-order model Markov model is employed since the imbalance evolution may depend on not only the previous state, but also on several n-steps before the state:

$$x_{t+r} = f_t(x_t, x_{t-r}, \cdots, x_{t-nr}) + u_t \tag{7}$$

where u_t is Gaussian white noise, f_t is the non-linear state transition function, x_{t+r} is the forecasting variable, r denotes

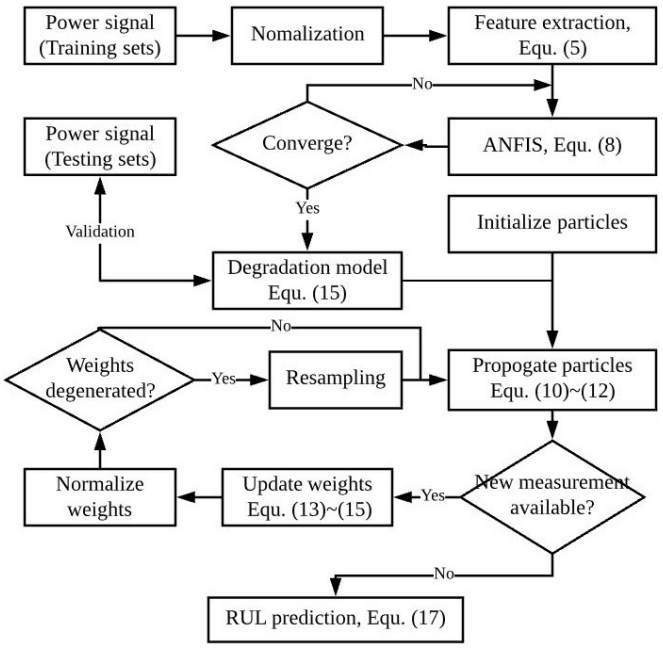

Fig. 1. Flowchart of the proposed framework for RUL prediction.

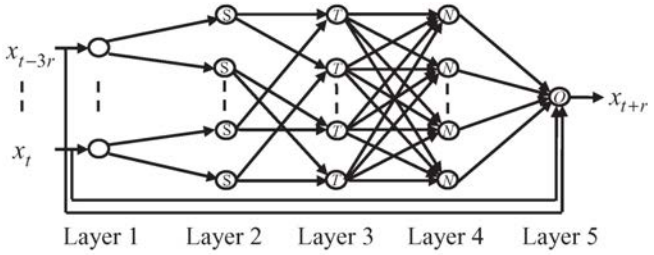

Fig. 2. The architecture of ANFIS [17].

the prediction step, and n defines the number of previous time steps. The architecture utilized in this paper is a five-layer ANFIS shown in Fig. 2, using 4th order Makov model (where $r = 1$, $n = 3$), with 16 fuzzy "*if-then*" learning rules based on first-order Sugeno model:

$$\begin{aligned} &IF\ (x_{t-3}\ is\ A_i^1)\ AND\ (x_{t-2}\ is\ A_i^2) \\ &\qquad AND\ (x_{t-1}\ is\ A_i^3)\ AND\ (x_t\ is\ A_i^4) \\ &THEN:\ x_{t+1}^i = w_1^i x_{t-3} + w_2^i x_{t-2} \\ &\qquad + w_3^i x_{t-1} + w_4^i x_t + w_5^i \\ &i = 1, 2, 3, ..., 16 \end{aligned} \tag{8}$$

where x_{t+1}^i is the output corresponding to the ith rule and A_i^j $(j = 1, 2, 3, 4)$ is the fuzzy set associated with the variables in the ith rule. $w_j^i (i = 1, 2, ..., 16)$ is the weight parameters corresponding to the jth input in the ith rule, determined by the learning process based on least-squares and the back propagation gradient descent method. Then calculate the final output x_{t+1} (state at time instant $t + 1$), which is the sum of all the outputs of each rule:

$$x_{t+1} = \sum_{i=1}^{16} x_{t+1}^i \tag{9}$$

B. Particle Filter for RUL PDF Estimation

The state estimation is achieved recursively in two steps: propagate and update. The propagate step is to obtain the prior PDF of the state for next time instant $k + 1$ by Chapman Kolmogorove equation:

$$p(x_{k+1}|z_{1:k}) = \int p(x_{k+1}|x_{k+1-n:k}) p(x_k|z_{1:k}) dx_k \tag{10}$$

where n is the order of Markov process; $p(x_{k+1}|x_{k+1-n:k})$ is the state transition probability defined via Equ. (5), reflecting the imbalance evolution process, and $p(x_k|x_{1:k})$ represents the state PDF at time k. Then the posterior state PDF can be calculated by:

$$p(x_{k+1}|z_{1:k+1}) = \frac{p(z_{k+1}|x_{k+1})}{p(z_{k+1}|z_{1:k})} p(x_{k+1}|z_{1:k}) \tag{11}$$

A sequential Monte Carlo method PF is adopted to approximate the posterior state PDF by a set of random particles with associated weights:

$$p(x_{k+1}|z_{1:k}) \approx \sum_{i=1}^{N} w_{k+1}^i \delta(x_{k+1} - \hat{x}_{k+1}^i) \tag{12}$$

where N is the total number of particles, $\hat{x}_{k+1}^i$ is the state value estimated by Equ. (5) of the ith particle at time $k + 1$, with associated weight w_{k+1}^i, and δ is the Dirac delta measure.

The update step is conducted when a new state measurement z_{k+1} is available. The weight of each particle is updated according to the importance sampling principle, followed by normalization so that weight sum is 1:

$$w_{k+1}^i \propto w_k^i p(z_{k+1}|\hat{x}_{k+1}^i) \tag{13}$$

where $p(z_{k+1}|\hat{x}_{k+1}^i)$ is Gaussian, with standard deviation of u_k in (5):

$$p(z_{k+1}|\hat{x}_{k+1}^i) = \frac{1}{\sqrt{2\pi}\mu_0} e^{\frac{-(z_{k+1} - \hat{x}_{k+1}^i)^2}{2\mu_0}} \tag{14}$$

Resampling is then performed to eliminate the particles with lowest weights, and a set of new particles is generated by duplicating the remaining particles. Since each particle is proportional to its weight so that the total number of particles is unchanged.

When there's no new measurement available, the update step of the PF cannot be conducted. Then, the propagate step of PF is implemented iteratively to calculate the prior PDF of the state at time instants to label the RUL. Each particle is updated recursively with a fixed state transition function trained by the available data of the fault feature NSR as:

$$\hat{x}_{k+m}^i = f_k(\hat{x}_{k+m-1}^i, \hat{x}_{k+m-2}^i, \hat{x}_{k+m-3}^i, \hat{x}_{k+m-4}^i) + u_{k+1} \tag{15}$$

Then, the prior PDF of the state at future time instants is used to estimate the RUL followed by:

$$p(x_{k+T}|z_{1:k}) = \int p(x_k|z_{1:k}) \prod_{g=k+1}^{k+T} p(x_g|x_{g-4:g-1}) dx_k \tag{16}$$

When the state of the ith particle at a future time instant $k+m$ reaches a threshold, the RUL is calculated by the particle to be the time between now and that future time instant, denoted as RUL_k^i. When all the particle reach the threshold, the PDF of the RUL $p(RUL_k|z_{1:k})$ at current time instant k can be obtained by:

$$p(RUL_k|z_{1:k}) = \sum_{i=1}^{N} w_k^i \delta(RUL_k - RUL_k^i) \qquad (17)$$

IV. EXPERIMENTAL RESULTS

A. Experimental Setup

In this paper, the dataset for evaluation of the proposed method is generated by a recently developed high-fidelity MHK simulation platform based on NREL's Fatigue, Aerodynamics, Structures, and Turbulence (FAST) code. In this simulation platform, the AeroDyn, ElastoDyn, ServoDyn and InflowWind modules are used with input parameters setting from a 20 kW MHK turbine located at the Southeast National Marine Renewable Energy Center (SNMREC). Stochastic turbulence models generated by NWTC's TurbSim platform is also utilized to provide realistic underwater operating environments. More details of the simulation platform and the parameters setting can refer to [18].

During the test, the hydrokinetic turbine was operated near a speed of 60 rpm, which corresponds to a fundamental rotating frequency $f = 1Hz$ (considered as healthy status). The blade imbalance fault is directly modeled by including an offset into the pitch angle of one rotor blade within FAST. When a blade imbalance fault occurs and develops, the vibration of the system will increase. This increased vibration will lead to the increase of the fault feature NSR, as well as the degradation of the turbine health condition and RUL reduction. To monitor the lifetime degradation process, we quantify the degradation into several periods associated with linearly accumulated pitch offset, 16 cases have been considered with pitch angle values from $0^\circ \sim 15^\circ$. This can represent an increased biofouling and corrosion of the blade in reality, which will cause imbalance to the system. In each pitch offset mode 10 intervals were set during the monitoring, and data were recorded for 120 seconds for each interval. As time progresses, the blade imbalance accumulated, along with the degradation of turbine until it reaches the threshold (set as failure status). A total of $16 \times 120 = 1920$ seconds data is recorded and 1500 seconds data is selected due to the instability at initial stage of simulation. The run-to-failure sensor records contain training datasets and testing datasets, collected at sampling rate $2/3Hz$ (1.5s/unit) under different fault levels. The training datasets and testing datasets were collected when the turbine simulated under the same average current velocity but different fluctuation (i.e. turbulent intensity of 5% and 10% separately) [18].

B. Results Analysis

Fig. 3 shows the DC-centered PSD spectrum near the fundamental frequency of the power signal when the blade is at different health conditions, $i.e.$, at different pitch angles of 0, 3, 6, 9, 12, 15 degrees. We can observe from the figure that when the blade enters the imbalance condition, the DC component (amplitudes of $0Hz$) is decreased significantly from 15.466 dB (0°) to 9.5608 dB (12°). The three main symmetric sidebands appear at the characteristic frequencies f_1, f_2, f_3 ($\pm 0.0195Hz$, $\pm 0.0293Hz$ and $\pm 0.0391Hz$). During the degradation, the amplitudes at $f_{1\sim3}$ change, and the sidebands of $0.5759Hz$ is restrained when pitch angle over 3°, new sidebands are excited at 0.0853. The results indicate that compared to the healthy state, more energy decreases at DC component ($0Hz$), along with energy changes at the sidebands of the power signal when the blade is in the imbalance fault condition.

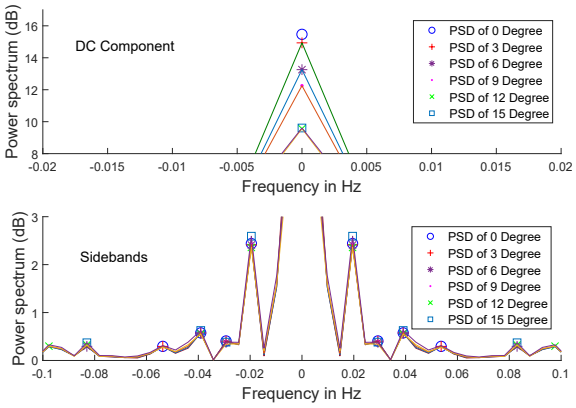

Fig. 3. DC-centered PSD of the power signal showing the DC component and its sidebands when the test blade is in the healthy and faulty condition

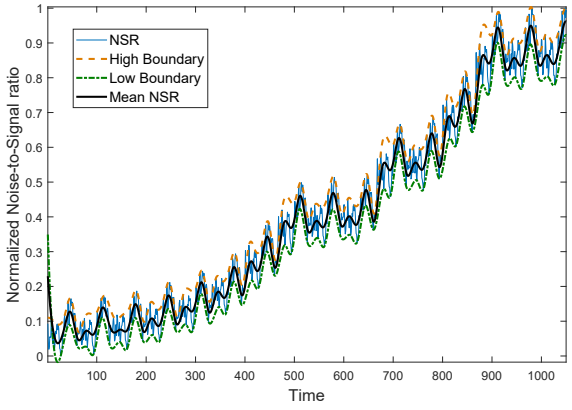

Fig. 4. Normalized NSR of the power signal during the run-to-failure experiments.

Fig. 4 shows the normalized NSR of the measured power signal during the entire run-to-failure experiments. In this paper, a Hilbert transform has been used to filter out the high frequency noise of the NSR obtained directly from the power signal, which has been chosen as a trade-off between the noise elimination and trend retention of the NSR. As Fig. 4 depicts, the NSR increases continuously during the degradation process, along with the increased pitch angle. The increase is stable at the beginning, and then accelerate when the pitch angle exceed 5° (associated with time at 400),

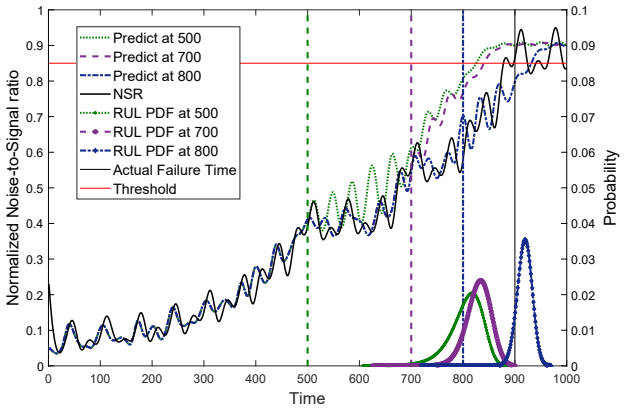

Fig. 5. Predicted PDFs of the RUL at different time instants calculated from Equ. (17).

then level off at a high value 0.85 when pitch angle reach at 12° (associated with time at 900). Therefore, the threshold indicates the end of the blade's life. The tendency of NSR verifies that it is an appropriate fault-related feature for fault prognosis.

Fig. 5 shows the PDF of the RUL prediction at time index of 500, 700, 800 using the proposed framework. The peak of each PDF curve represents the highest probability of the predicted failure time. According to Fig. 5, more particles predict the RUL gathering to the peak of PDF as time goes on. The peak of the PDF predicted at 800 is closed to 900, which is the actual failure time when the NSR reaches 0.85, indicating that the RUL prediction precise has positive correlation with the time. The reason lies in is that the ANFIS and PF methods have the ability to use new fault features to improve its accuracy in the RUL prediction as time goes on.

V. Conclusions and Future Work

This paper proposed a RUL prediction framework for MHK turbine blade under imbalance fault based on ANFIS and PF approaches. Considering the fault information is typically weak in the generator power signal, a novel NSR based on the power signal was defined for fault feature extraction, which was then trained to model the blade imbalance fault propagation trend. Additionally, the PF algorithm was implemented to predict the RUL PDF of the turbine blade based on the learned degradation model using ANFIS and the fault feature. Experimental datasets collected from a high-fidelity simulated MHK turbine subjected to blade imbalance faults were used to evaluate the performance of the proposed framework. Results have shown that the proposed method can effectively obtain the RUL of the turbine blade, and the prediction becomes more and more accurate as time goes on.

Future work will focus on testing the proposed framework on other MHK generation system failures, such as the drivetrain system and gearbox failures. Additionally, the ANFIS will be compared with deep learning methods, such as the deep recurrent neural network (RNN), for more robust and efficient fault prognostic and RUL estimation.

Acknowledgment

This work was supported by the National Science Foundation under grant ECCS-1809164 and the National Science Foundation of China under grant 61803329. We would like to thank Drs. Hassan Mahfuz and Takuya Suzuki for providing our team with their FAST models, and Broc Dunlap and David Wilson for preparing the TurbSim and simulation data.

References

[1] S. Dolman and M. Simmonds, "Towards best environmental practice for cetacean conservation in developing scotland's marine renewable energy," *Marine Policy*, vol. 34, no. 5, pp. 1021–1027, 2010.

[2] J. R. Haslett, M. Garcia-Llorente, P. A. Harrison, S. Li, and P. M. Berry, "Offshore renewable energy and nature conservation: the case of marine tidal turbines in northern ireland," *Biodiversity and Conservation*, vol. 27, no. 7, pp. 1619–1638, 2018.

[3] D. B. Jarrell, D. R. Sisk, and L. J. Bond, "Prognostics and condition-based maintenance: a new approach to precursive metrics," *Nuclear technology*, vol. 145, no. 3, pp. 275–286, 2004.

[4] D. Banjevic, "Remaining useful life in theory and practice," *Metrika*, vol. 69, no. 2-3, pp. 337–349, 2009.

[5] X.-S. Si, W. Wang, C.-H. Hu, and D.-H. Zhou, "Remaining useful life estimation–a review on the statistical data driven approaches," *European journal of operational research*, vol. 213, no. 1, pp. 1–14, 2011.

[6] J. Sikorska, M. Hodkiewicz, and L. Ma, "Prognostic modelling options for remaining useful life estimation by industry," *Mechanical Systems and Signal Processing*, vol. 25, no. 5, pp. 1803–1836, 2011.

[7] Y. Lei, N. Li, L. Guo, N. Li, T. Yan, and J. Lin, "Machinery health prognostics: A systematic review from data acquisition to rul prediction," *Mechanical Systems and Signal Processing*, vol. 104, pp. 799–834, 2018.

[8] C. Ordóñez, F. S. Lasheras, J. Roca-Pardiñas, and F. J. de Cos Juez, "A hybrid arima–svm model for the study of the remaining useful life of aircraft engines," *Journal of Computational and Applied Mathematics*, vol. 346, pp. 184–191, 2019.

[9] Y. Qian, R. Yan, and R. X. Gao, "A multi-time scale approach to remaining useful life prediction in rolling bearing," *Mechanical Systems and Signal Processing*, vol. 83, pp. 549–567, 2017.

[10] X. Li, Q. Ding, and J.-Q. Sun, "Remaining useful life estimation in prognostics using deep convolution neural networks," *Reliability Engineering & System Safety*, vol. 172, pp. 1–11, 2018.

[11] Z. Tian, "An artificial neural network method for remaining useful life prediction of equipment subject to condition monitoring," *Journal of Intelligent Manufacturing*, vol. 23, no. 2, pp. 227–237, 2012.

[12] B. Y. Bejarbaneh, E. Y. Bejarbaneh, A. Fahimifar, D. J. Armaghani, M. Z. A. Majid *et al.*, "Intelligent modelling of sandstone deformation behaviour using fuzzy logic and neural network systems," *Bulletin of Engineering Geology and the Environment*, vol. 77, no. 1, pp. 345–361, 2018.

[13] A. Soualhi, M. Makdessi, R. German, F. R. Echeverría, H. Razik, A. Sari, P. Venet, and G. Clerc, "Heath monitoring of capacitors and supercapacitors using the neo-fuzzy neural approach," *IEEE Transactions on Industrial Informatics*, vol. 14, no. 1, pp. 24–34, 2018.

[14] F. Cheng, L. Qu, and W. Qiao, "Fault prognosis and remaining useful life prediction of wind turbine gearboxes using current signal analysis," *IEEE Transactions on Sustainable Energy*, vol. 9, no. 1, pp. 157–167, 2018.

[15] N. Li, Y. Lei, J. Lin, and S. X. Ding, "An improved exponential model for predicting remaining useful life of rolling element bearings," *IEEE Transactions on Industrial Electronics*, vol. 62, no. 12, pp. 7762–7773, 2015.

[16] E. Muljadi and Y.-H. Yu, "Review of marine hydrokinetic power generation and power plant," *Electric Power Components and Systems*, vol. 43, no. 12, pp. 1422–1433, 2015.

[17] J.-S. Jang, "Anfis: adaptive-network-based fuzzy inference system," *IEEE transactions on systems, man, and cybernetics*, vol. 23, no. 3, pp. 665–685, 1993.

[18] Y. Tang, J. VanZwieten, B. Dunlap, D. Wilson, C. Sultan, and N. Xiros, "In-stream hydrokinetic turbine fault detection and fault tolerant control - a benchmark model," in *American Control Conference (ACC), 2019*. IEEE, 2019 (Submitted).